Nitrogen cycling and bacterial community structure of sinking and aging diatom aggregates

Ann Sofie Birch Lundgaard[1],*, **Alexander H. Treusch[1], Peter Stief[1], Bo Thamdrup[1], Ronnie N. Glud[1,2,3]**

[1]Department of Biology and Nordic Center for Earth Evolution, University of Southern Denmark, 5230 Odense M, Denmark
[2]Scottish Association for Marine Science, Scottish Marine Institute, Oban PA37 1QA, UK
[3]Department of Ocean and Environmental Sciences, Tokyo University of Marine Science and Technology, Tokyo 108-8477, Japan

ABSTRACT: Sinking phycodetrital aggregates can contribute to anaerobic nitrogen turnover as they may represent oxygen-depleted microbial hot spots in otherwise oxygenated waters. However, the dynamics of anaerobic nitrogen cycling during the long descent of aggregates through oxic or hypoxic waters are unknown. Thus, model aggregates prepared from the diatom *Skeletonema marinoi* were allowed to age for 4 d at high and low ambient O_2 levels (70 and 15% air saturation, respectively), and changes in nitrogen transformations and microbial community structure were followed. At both O_2 levels, denitrification and dissimilatory NO_3^- reduction to NO_2^- (DNRN) were the most important processes of aggregate-associated anaerobic nitrogen cycling. However, at 70% air saturation, rates of anaerobic N cycling were lower and decayed towards 0 after an early rise, whereas at 15% air saturation, they remained constantly high at average production rates of 0.66 nmol N_2-N aggregate (aggr.)$^{-1}$ h^{-1} and 0.26 nmol NO_2^- aggr.$^{-1}$ h^{-1}. At both O_2 levels, but more pronouncedly at 70% air saturation, the microbial community underwent succession as expressed by an increase in (1) relative abundance of specific bacterial taxonomic units; (2) bacterial diversity; and (3) prokaryotic abundance. Probably, a higher carbon oxidation rate at high ambient O_2 level progressively selected for microbes capable of using complex carbon polymers. Taken together, the occurrence of anoxic aggregate centers may be ephemeral at high ambient O_2 levels, but persistent at low ambient O_2 levels, indicating that sinking phycodetrital aggregates can remain sinks for bioavailable N in the oceans for several days, especially in O_2-depleted settings.

KEY WORDS: Marine snow · Diatom aggregates · Nitrogen cycle · Denitrification · ^{15}N-labeling experiments · Oxygen minimum zone · Molecular community fingerprinting

INTRODUCTION

Sinking macroscopic aggregates represent an important conduit for transferring organic material and nutrients from the photic zone to deeper waters, and are a ubiquitous feature of most marine settings. However, their formation is particularly intensive at the end of phytoplankton blooms and in polar regions during periods of sea-ice melt, which can lead to mass release of agglutinated sea-ice algae (Smetacek 1985, Boetius et al. 2013, Fernández-

Méndez et al. 2014, Glud et al. 2014). Although typically dominated by algal material, aggregates also include zooplankton carcasses, protists, fecal pellets, and detrital particles in different stages of decomposition (Silver 2015). 'Marine snow' thus consists of highly diverse microhabitats that sink towards the seabed. The diameter of macroscopic aggregates ranges from 500 µm to several centimeters (Simon et al. 2002, Grossart et al. 2003, Glud et al. 2014) and their sinking velocity reaches up to several hundred meters per day, depending on the size and density of

*Corresponding author: aslundgaard@biology.sdu.dk

the aggregates (Simon et al. 2002, Ziervogel & Forster 2005, Iversen & Ploug 2013, Agusti et al. 2015). The sinking aggregates generally exhibit intensified metabolic activity (Ploug & Grossart 2000, Grossart & Ploug 2001) and function as metabolic hot spots with microbial densities that are 3 to 4 orders of magnitude larger than in the ambient water (Wörner et al. 2000, Silver 2015, Thiele et al. 2015). The aggregate-associated microbial communities are also typically fundamentally different from those of the surrounding seawater (Alldredge & Youngbluth 1985, DeLong et al. 1993, Moeseneder et al. 2001).

One important aspect of sinking aggregates is the possibility to form anoxic centers hosting active anaerobic microbial communities. This has been documented for compact fecal pellets (Alldredge & Cohen 1987), zooplankton carcasses (Glud et al. 2015), cyanobacterial colonies and aggregates (Paerl & Bebout 1988, Klawonn et al. 2015), and diatom aggregates (Ploug et al. 1997, Ploug & Bergkvist 2015, Stief et al. 2016). Recent investigations documented denitrification and dissimilative nitrate reduction to ammonia (DNRA) activity in sinking diatom and cyanobacterial aggregates being exposed to low ambient O_2 levels (<40% air saturation [AS]) (Klawonn et al. 2015, Ploug & Bergkvist 2015, Stief et al. 2016). Thus, sinking phycodetrital aggregates can potentially play an important role for N turnover in the pelagic environment, especially if they contain diatoms that have NO_3^- storing capabilities (Stief et al. 2016, Kamp et al. 2016).

Sinking aggregates are, however, not static microenvironments and their dynamic nature needs to be acknowledged to assess their potential impact on pelagic N cycling. Availability of labile organic material, nutrients, and O_2 will change in response to ongoing metabolic activity, cell lysis, and microbial succession within the aging aggregates. Furthermore, these processes will interrelate with the ambient concentrations of O_2 and NO_3^-, and respond to changes in temperature. The changing internal microenvironment is expected to affect the relative importance and the coupling between N transformations, such as nitrification, denitrification, and DNRA — and thereby the products of N processing associated with sinking aggregates. However, investigations of any succession in N processing and microbial community structure in aging aggregates have not been conducted in detail. To assess the potential importance of sinking aggregates for pelagic N cycling, it remains to be investigated whether anaerobic N cycling persists for longer periods or represents only a short incidental period during aggregate descend. The present study aimed to quantify the development in nitrogen turnover of sinking and aging model aggregates dominated by the ubiquitous diatom *Skeletonema marinoi*. Specific process rates were followed for a total of 4 d through $^{15}NO_3^-$ enrichment incubations at 2 different ambient O_2 levels. Concurrently, the succession in microbial community size and structure within the aggregates was followed in order to reveal potential links to community metabolism. The combined data were used to evaluate and discuss the potential importance of sinking diatom aggregates for N turnover in the oceans, with particular emphasis on areas with reduced O_2 levels.

MATERIALS AND METHODS

Production of model aggregates

Diatom-based aggregates were produced from an axenic culture of the marine diatom *Skeletonema marinoi* (CCMP1332, NCMA). For aggregate production, culture samples were mixed with unfiltered preconditioned coastal surface seawater collected near Kerteminde, Denmark (55° 27′ 00.5″ N, 10° 39′ 44.1″ E). Preconditioning of the water included raising the *in situ* salinity from 23 to 30 with NaCl to match the growth conditions of the *S. marinoi* strain used, and incubation at 15°C for 2 wk prior to aggregate production to allow the bacterial community to adapt to the higher salinity.

Aggregate production was initiated by mixing 45 ml of stationary-phase *S. marinoi* culture and 585 ml seawater into gas-tight glass bottles, avoiding entrapment of gas bubbles. In total, 28 bottles were mounted on a plankton wheel with a diameter of 70 cm rotating at 1.7 rpm. The rotating bottles were kept in a 12 h light:12 h dark cycle at 15°C. Visual aggregates appeared within the first hour, and within 3 d, the ellipsoid-shaped aggregates (Fig. 1A,C) had a rather uniform size of 2.2, 1.6, and 1.6 mm in length, height, and width, respectively, and a volume of 3.1 mm³ ± 1.3 (mean ± SE; n = 48). These freshly formed aggregates were then used for the succession experiment.

Succession experiment

Intact, similar sized aggregates were carefully transferred from the production bottles to new 0.5 l glass bottles containing seawater, using a glass tube (10 cm long, 0.5 cm in inner diameter) equipped with
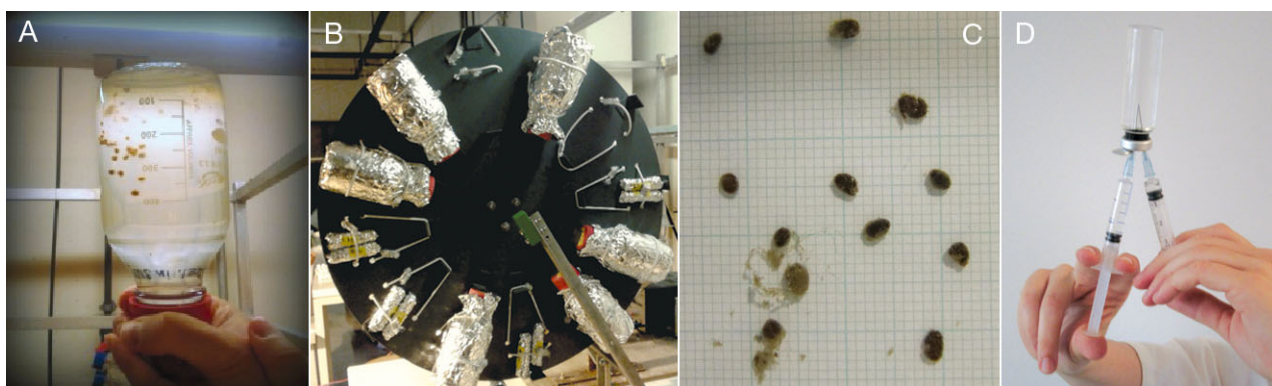
Fig. 1. (A) A production bottle and (B) storage bottles on a plankton wheel with (C) *Skeletonema marinoi* aggregates. (D) Sampling of water during the short-term ^{15}N-enrichment experiments. One syringe contained $^{15}NO_3^-$-enriched replacement water with an O_2 concentration that would counteract the concentration drop in the vial, and was injected as the sample water was withdrawn by the empty syringe

a syringe for suction. The seawater was enriched with NO_3^- to a final concentration of 25 µM (comparable to nitrate concentrations in typical deeper, oceanic water) (Anderson et al. 1982, Codispoti et al. 2001). A total of 11 aggregates were transferred to each bottle and 18 bottles were prepared in all. In each incubation bottle, all aggregates came from different production bottles. In total, 9 bottles were adjusted to low O_2 conditions (i.e. 15% AS), and 9 bottles were adjusted to high O_2 conditions (i.e. 70% AS) by flushing with O_2 and N_2 as controlled by a digital gas mixer (Brooks Mass Flow Controller). The closed incubation bottles were incubated on the plankton wheel in darkness at 15°C for 4 d (Fig. 1B). Oxygen concentration was monitored over time with custom-made O_2-sensitive fluorescent patches, fixed to the inside of the bottles (Glud et al. 2015). The sensor patches were interrogated from the outside by a FireStingO$_2$ meter (Pyro Science). A large fraction of the seawater was exchanged twice per day to maintain almost constant O_2 concentration (±6 and 29% of the set point values in the high and low O_2 treatments, respectively) and to renew the natural constituents of the seawater (e.g. dissolved organic carbon [DOC], nutrients, small particles, and bacteria). After 1 d of incubation (designated T_{1d}), 6 bottles (3 from the low and 3 from the high O_2 treatment) were sacrificed for rate measurements of key processes of the nitrogen cycle, characterization of the microbial communities, and enumeration of prokaryote abundance. This was repeated 2 (T_{2d}) and 4 d (T_{4d}) after initiating the experiment. A common reference point for both oxygen treatments was included by initial sampling of aggregates prior to any O_2 treatments (T_{0d}).

Measurement of N cycle processes

Experimental procedure

The most relevant dissimilatory processes of the nitrogen cycle were measured in short-term (6 h) ^{15}N isotope enrichment incubations. At each sampling point (i.e. T_{0d}, T_{1d}, T_{2d}, and T_{4d}), 8 intact aggregates were transferred from each glass bottle (3 from the low and 3 from the high O_2 treatment) to a 20 ml glass vial filled with seawater and equipped with an oxygen optode patch. The 3 remaining aggregates in each bottle were sampled for microbial community structure. The seawater was enriched with 25 µM $^{15}NO_3^-$ and the O_2 AS level was adjusted to 15 or 70% (corresponding to 39 or 183 µM, respectively) by flushing with O_2 and He as controlled by a digital gas mixer. For controls, 2 vials without aggregates were incubated in parallel under the same conditions at 15 and 70% O_2 AS, respectively. The background NO_3^- concentration in the aged seawater was 3.7 µM (corresponding to 13% of total NO_3^- after $^{15}NO_3^-$ addition). The vials were sealed with gas-tight stoppers avoiding entrapment of gas bubbles, and were incubated on the plankton wheel (1.7 rpm) in darkness at 15°C for 6 h. After 0, 1, 2, 4, and 6 h, O_2 was measured and a water sample (3 ml) was taken from each glass vial. On each occasion, the water withdrawn from the glass vial was replaced with $^{15}NO_3^-$-enriched seawater adjusted to an O_2 concentration that would compensate for the drop in O_2 concentration since the last sampling point (Fig. 1D). The 3 ml sample was split into the following 2 vials: (1) 1.5 ml was added to 3 ml He-flushed, half-evacuated Exetainers (Labco) containing 50 µl $ZnCl_2$ (50%) and

stored for ^{15}N analysis; and (2) the remaining 1.5 ml was stored at −20°C for dissolved inorganic nitrogen (DIN) analysis as described by Stief et al. (2016).

Nitrogen analyses

NO_3^- and NO_2^- concentrations were quantified on a NOx analyzer (CLD 66s, Eco Physics) with the VCl$_3$ and NaI reduction assay, respectively (Braman & Hendrix 1989, Yang et al. 1997). NH_4^+ concentrations were determined with the Na-salicylate method (Bower & Holm-Hansen 1980) using a spectrophotometer (Multiskan GO Microplate spectrophotometer, Thermo Scientific). Isotopically labeled nitrogen species ^{15}N-N$_2$ (^{29}N$_2$ + ^{30}N$_2$), ^{15}NO$_2^-$, and ^{15}NH$_4^+$ were analyzed on a gas chromatography-isotopic ratio mass spectrometer (GC-IRMS; Thermo Delta V Plus, Thermo Scientific) (Dalsgaard et al. 2012). The samples for N$_2$ analysis were withdrawn from the headspace of the 3 ml Exetainers, while ^{15}N-labeling of NO$_2^-$ and NH$_4^+$ was analyzed with the sulfamic acid and the hypobromite assay, respectively, followed by measurement of ^{15}N-N$_2$ (Warembourg 1993, McIlvin & Altabet 2005, Stief et al. 2016). Accumulation of ^{15}N$_2$O was not detected in any of the incubations.

Aggregate characterization

For quantification of the C:N ratio, aggregates (from short-term incubations at T_{0d}) were filtered (with deionized water) onto pre-weighed, combusted 25 mm GF/F filters. The filter-samples were dried for 2 d at 60°C and analyzed on a Carlo-Erba CHN analyzer. The sinking speeds of 19 aggregates from another batch of aggregates with similar dimensions were visually determined in a sedimentation column (mean diameter [∅] = 2.7cm) at 14°C and salinity of 30. The excess density at the experimental conditions was calculated from the sinking speeds using the Navier–Stokes drag equation according to Iversen & Ploug (2010).

Rate calculations and statistics

The rate of solute production and consumption was calculated from linear regression of concentration changes during the incubations, accounting for any dilution during the sampling process. As the rates measured in the water with aggregates included any activity from the free-living microbial community, the control rates were subtracted to derive the aggregate-specific rates of the respective solutes.

The slope of each replicate and the mean slopes were analyzed with t-tests (2-tailed and 1-tailed, respectively) to test whether they were significantly different from 0. The effect of time on the same variables in either the high or low O$_2$ treatment was tested with ANOVA (1-way) and Tukey post hoc tests were performed in R (R core team, version 3.1.2). The effect of time was further tested by plotting the replicate rates with time (4 d) and analyzing the regressions with t-tests (2-way).

The production/consumption of N compounds was integrated over the 4 d of aging to derive a time-integrated turnover, and standard error was calculated according to the rules of error propagation. The effect of O$_2$ on the time-integrated turnover was tested with t-tests (2-tailed). The total N$_2$ produced from denitrification was calculated using the relation between the ^{29}N$_2$ and ^{30}N$_2$ production rates, assuming random isotope pairing. The calculations accounted not only for the background ^{14}NO$_3^-$, but also for other possible sources of ^{14}NO$_3^-$, for example from nitrification and leakage of intracellular nitrate from *S. marinoi* (Kamp et al. 2011, Stief et al. 2016).

Microbial community analysis

Enumeration of prokaryotes

Immediately after the short-term incubations, aggregate samples for prokaryotic abundance were disintegrated to detach aggregate-associated prokaryotes. The aggregates were exposed to ultra-sonication (Branson 2200, 60 W, 160 s) in 0.025 mM tetrasodium pyrophosphate fixed with paraformaldehyde to 2% final concentration (Velji & Albright 1986, Schramm et al. 1998), and stored at 4°C until enumeration. For counting prokaryotes, the preserved samples (in triplicates) were diluted and filtered onto 0.2 µm Nuclepore track-etched membranes (Whatman, GE Healthcare) followed by staining with 4′,6-diamidino-2-phenylindole (DAPI). The prokaryotes were hereafter visualized with an epifluorescence microscope where 10 fields of view were counted for each sample (to include >500 cells in each count).

DNA extraction and bacterial community profiling

From each oxygen treatment and respective sampling points, 3 aggregates were pooled into UV-

sterilized cryo vials, and were immediately frozen in liquid nitrogen before being stored at $-80°C$ until DNA extraction. The aged seawater, the seawater from the aggregate production bottles, and the seawater from the succession experiment were filtered (0.5 l) onto sterile 0.2 µm Supor 200 polyethersulfone membranes (Pall Corporation, Life Sciences) and stored like the aggregate samples. The DNA extractions from the aggregate and the water samples were performed using the PowerLyzer PowerSoil DNA Isolation Kit and the PowerWater DNA Isolation Kit, respectively (both MO BIO), following the manufacturer's protocol. The DNA was quantified with a fluorometer with the Quant-iT PicoGreen Kit (Invitrogen), providing average yields of 5.1 and 32.3 ng µl^{-1} in the solution for aggregates and water, respectively.

To profile the bacterial community with terminal restriction length polymorphism (T-RFLP) analysis (Liu et al. 1997), the genes encoding bacterial 16S rRNA were amplified with PCR using the phosphoramidite fluorochrome 5-carboxyfluorescein labeled forward primer B27FAM (50-AGR GTT YGA TYM TGG CTC AG-30) and the reverse primer U519R (50-GWA TTA CCG CGG CKG CTG-30). PCR was performed in 50 µl reactions with final amounts of 5 to 10 ng template, 20 pmol of each primer, 10 nmol deoxynucleoside triphosphates in equal amounts, 5 µl 10X *Taq* buffer with $(NH_4)_2SO_4$, 1.25 units *Taq* polymerase, and 125 nmol $MgCl_2$ (all Thermo Scientific). Denaturation at 94°C for 2 min was followed by 32 cycles of 94°C for 20 s, 54°C for 45 s, and 72°C for 45 s, with a final elongation step of 5 min at 72°C. Successful amplification was verified by agarose gel electrophoresis using 1.5% gels. The ~500 bp PCR product was incubated with 5 U of the restriction enzyme *Bsu*RI in buffer R (Thermo Scientific) at 37°C for 12 h, followed by heat inactivation at 80°C for 20 min. Resulting restriction fragments were purified with the GeneJET PCR purification kit (Thermo Scientific). The average DNA yield after PCR, restriction, and purification was 4.2 ng µl^{-1}. Finally, the processed DNA (~100 ng) was analyzed with capillary electrophoresis at the Uppsala Genome Center in Sweden.

Bioinformatics analysis of the microbial community profiles

For sizing, the T-RFLP data were analyzed with the Peak Scanner software (Applied Biosystems). Noise filtration, clustering, and construction of data matrices were performed with the online program T-RFLP analysis EXpedited (http://trex.biohpc.org/) with a noise filtration factor of 1.2 based on the peak area, and a clustering threshold factor of 0.5. The operational taxonomic unit (OTU) fluorescence was standardized to the total fluorescence of all OTUs in a sample, and matrices of different sample combinations of interest were created. For each of these matrices, only OTUs with a relative abundance above 0.5% and those present in more than 1 sample were analyzed. The data matrices were analyzed with R (R core team, version 3.1.2) and the R package vegan (Oksanen et al. 2013), where the dissimilarities between samples and their respective OTUs were calculated and visualized with non-metric multidimensional scaling (NMDS). The function metaMDS was used to find the best fit between Bray-Curtis dissimilarities and ordinations with minimal stress (goodness of fit). Owing to a large range, the data values were square-root transformed, and then submitted to Wisconsin double standardization. The function found species scores as weighted averages of site scores, but expanded them so that species and site scores had equal variances (Oksanen et al. 2013). All NMDS settled for 2 dimensions and low stress ranging from 0.06 to 0.1, also evaluated with Shepard plots. Relevant environmental data were fitted onto the ordination with the function envfit, where the projection of points has maximum correlation with corresponding environmental variables (Oksanen et al. 2013). Analysis of similarities (ANOSIM) was used to test statistically whether there was a significant difference between sample groups of interest (Oksanen et al. 2013).

RESULTS

Aggregate characteristics

During aggregate formation, the O_2 concentration in the production bottles increased during daytime to ~110% AS. Hence, O_2 production by the viable diatoms exceeded O_2 consumption by microbial respiration under light conditions. However, during the 4 d succession experiment in darkness, the O_2 concentration declined, and water was exchanged twice a day to maintain stable O_2 concentrations in the bottles, with means of 17.8 ± 0.6 and 67.3 ± 0.6% AS (mean ± SE, n = 65) in the low and high O_2 treatments, respectively. No measurable change in aggregate size during the incubation was detected, and the ellipsoidal aggregates maintained the average diameters of 2.2 ± 0.1, 1.6 ± 0.1, and 1.6 ± 0.1 mm corresponding to a volume of 3.1 ± 0.2 mm^3 (n = 45). The

average molar C:N ratio of the aggregates was 7.3 ± 0.2 (n = 5) and the average sinking speed of the aggregates amounted to 374 ± 28 m d^{-1} (n = 19), which equates to an excess density of 2.6 µg cm^{-3}.

Aggregate-associated O_2 respiration and N cycling

The metabolic activity of the aggregates was quantified at 4 time points during the 4 d succession experiment. Generally, the solute concentrations changed linearly over the 6 h incubations (after correction for dilution during sampling) (Fig. 2; see Fig. S1 in the Supplement at www.int-res.com/articles/suppl/a079p085_supp.pdf). Only in a few instances did the solute concentration change non-linearly, e.g. the N_2 production in the low O_2 treatment accelerated towards the end of the T_{0d} incubation (Fig. 2B). This was probably due to the transfer of aggregates directly from the production bottles kept at ~100% O_2 AS to the incubation bottles with 15%

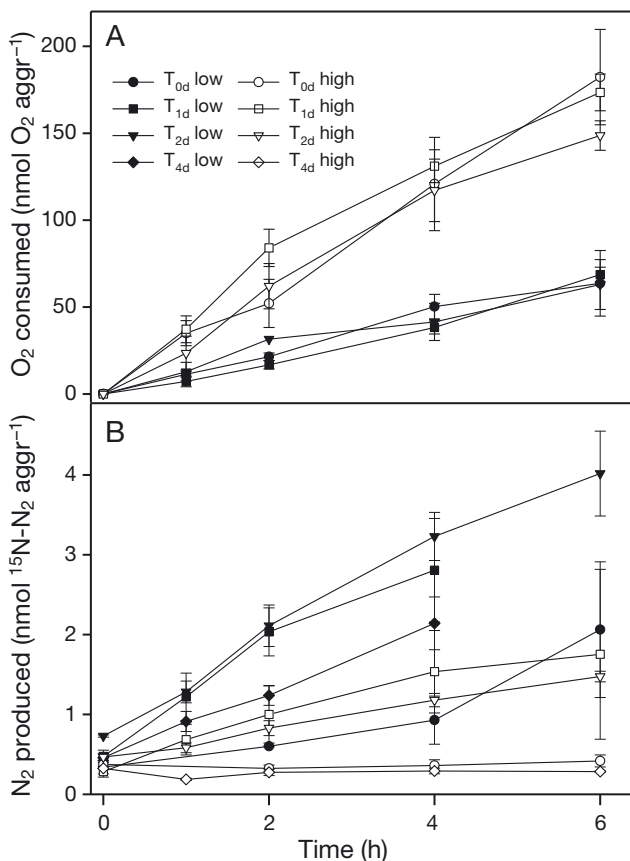Fig. 2. Time series (mean ± SE, n = 3) of (A) the O_2 consumed and (B) the ^{15}N-N_2 produced by sinking *Skeletonema marinoi* aggregates during short-term incubations at either 15% (low) or 70% (high) O_2 AS at T_{0d}, T_{1d}, T_{2d}, and T_{4d}. Owing to technical problems, there are no O_2 data available for Day 4

O_2 AS, which must have reduced the internal O_2 availability. However, active denitrification might have to await production of required enzymes and thus exhibit a lag phase. Remarkably, there was no statistical significant change in the consumption rates of O_2 during the 2 d study period (O_2 data for Day 4 are missing due to instrument failure), or NO_3^- during the 4 d study period, in either of the 2 treatments. The O_2 respiration rate measured in seawater without aggregates (i.e. in control incubations) corresponded to 48 ± 1.2 and 40 ± 12% of the total O_2 respiration rate in the high and low O_2 treatment with aggregates, respectively. This corresponds to a 1000-fold lower volume-specific activity in the water as compared to the aggregate. On average, aggregates consumed 10.4 ± 0.1 nmol O_2 aggr.$^{-1}$ h^{-1} (n = 12) in the low O_2 treatment. This was less than half the consumption of 28.7 ± 0.2 nmol aggr.$^{-1}$ h^{-1} in the high O_2 treatment (Fig. 3A). The difference presumably reflects the different oxic volumes of the aggregates in the respective treatments. Concurrently, the average nitrate consumption rates over the 4 d were 1.15 ± 0.02 and 0.31 ± 0.02 nmol N aggr.$^{-1}$ h^{-1} in the low and the high O_2 treatments, respectively (Fig. 3B), while control incubations without aggregates exhibited no significant change in the ambient NO_3^- concentrations (not shown).

Nitrite and N_2 were produced from NO_3^- reduction in most incubations (Fig. 3C,D). In the low O_2 treatment, the production rate of the reduced nitrogen compounds remained fairly constant throughout the study period (Fig. 3C,D, Table S2), with average values of 0.26 ± 0.003 and 0.66 ± 0.01 nmol N aggr.$^{-1}$ h^{-1} for NO_2^- and N_2, respectively (Fig. 3C,D). In contrast, the high O_2 treatment exhibited a maximum in N_2 and NO_2^- production at T_{1d}, followed by a statistically significant gradual decline towards 0 at the end of the experiment (Fig. 3C,D). The maximum rates amounted to 0.09 ± 0.04 and 0.37 ± 0.12 nmol N aggr.$^{-1}$ h^{-1} for NO_2^- and N_2, respectively; however, they were still markedly lower than those encountered during the low O_2 treatments (Fig. 3C,D, Tables S1 & S2). The $^{15}NH_4^+$ accumulation rate was in the very low range (<pmol aggr.$^{-1}$ h^{-1}) and the total NH_4^+ concentrations remained below the detection limit of 0.4 µM of the salicylate method (Kempers & Kok 1989), indicating only insignificant DNRA activity in the investigated aggregates. No ^{15}N-N_2O production was detected in any incubations (detection limit ~0.2 nM N aggr.$^{-1}$ h^{-1}).

To overcome any bias introduced during aggregate production, we selected aggregates from different production bottles and pooled 8 in each incubation. However, parallel incubations still exhibited consid-
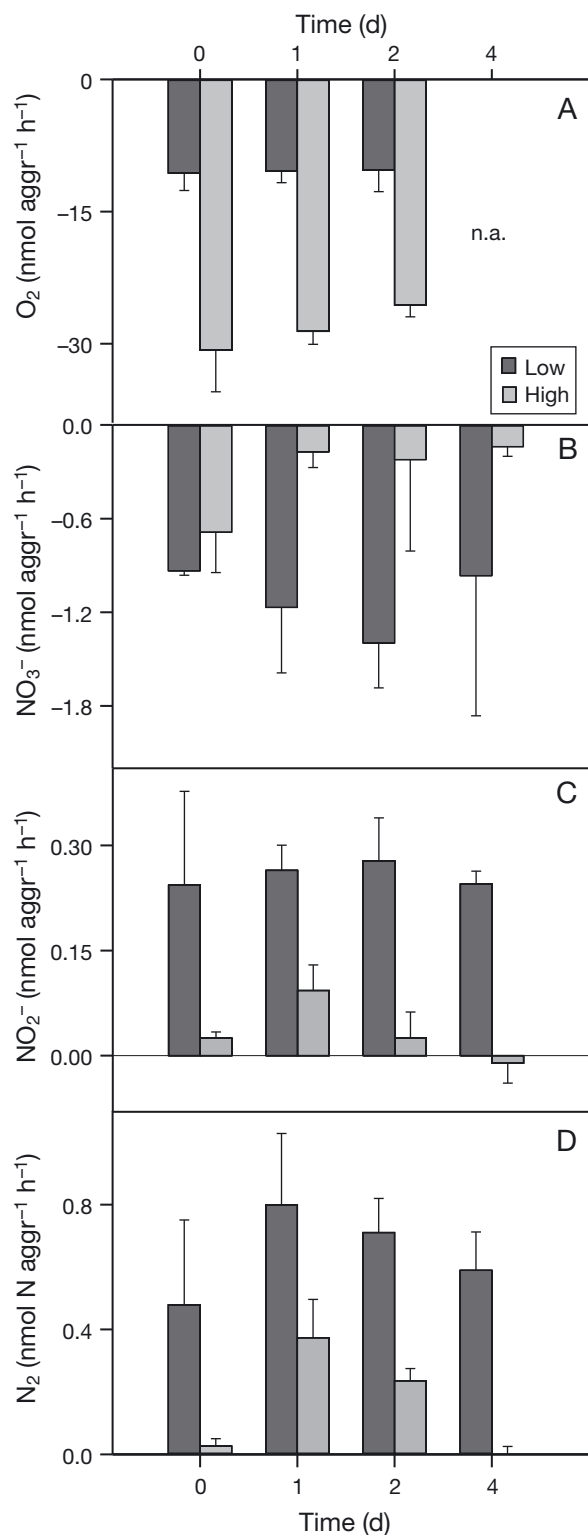
Fig. 3. Aggregate-specific rates (mean ± SE, n = 3) of (A) O_2, (B) NO_3^-, (C) NO_2^-, and (D) N_2 of sinking S*keletonema marinoi* aggregates at 15% (Low) and 70% (High) O_2 AS during a 4 d period. Positive and negative rates correspond to production and consumption, respectively. Owing to technical problems, there are no O_2 data available (n.a.) for Day 4

erable variations, reflecting relatively high heterogeneity among aggregates. For instance, in the high O_2 treatment, at T_{1d}, each replicate exhibited statistically significant total N_2 production (0.09, 0.37, and 0.32 nmol N aggr.$^{-1}$ h^{-1}), but the mean of the 3 was not significantly different from 0. Only at T_{2d} was the average value significantly different from 0 (N_2 total: 0.24 ± 0.04 nmol N aggr.$^{-1}$ h^{-1}) (Table S1). In the low O_2 treatment, the means of N_2 total production were significantly different from 0 in all instances, with the exception of T_{0d}. Thus, the data confirm N_2 production in aggregates in both O_2 treatments, but with highly variable rates between different incubations. The production ratio of $^{29}N_2$ ($^{14}N^{15}N$) and $^{30}N_2$ ($^{15}N^{15}N$) was slightly higher than predicted from the ^{15}N labeling fraction of NO_3^-, and $^{28}N_2$ ($^{14}N^{14}N$) was estimated to account for 21 to 31% of total N_2 production assuming random isotope paring (Nielsen 1992, Stief et al. 2016). Thus, 87 ± 9 and 92 ± 10% of the ^{14}N-N_2 production could be explained from the $^{14}NO_3^-$ background in the seawater in the low and the high O_2 treatments, respectively, based on the isotopes pairing calculations in N_2.

Time-integrated O_2 and N turnover

The time-integrated O_2 consumption in the high O_2 treatment was ~3 times higher than in the low O_2 treatment, while the consumption of NO_3^- was ~4 times higher in the low O_2 treatment. Correspondingly, the time-integrated productions of NO_2^- and N_2 were ~8 and ~4 times higher in the low O_2 treatment, respectively (Fig. 4). The effect of ambient O_2 was statistically significant for consumption rates of NO_3^-, and production rates of NO_2^- and N_2 (Table S2). This strongly indicates a regulatory role of the ambient O_2 levels for the interior microbial mediated processes and pathways within the aggregates. The N budget was not completely closed, as 20 and 11% of total NO_3^- consumption was not balanced by the concurrent production of NO_2^- and N_2 in the low and high O_2 treatments, respectively (Fig. 4). The difference could partly be related to N assimilation by the fast-growing aggregate-associated microbes.

Prokaryotic abundance and bacterial community structure

The abundance of aggregate-associated prokaryotes increased with an initial doubling time of 25 h in
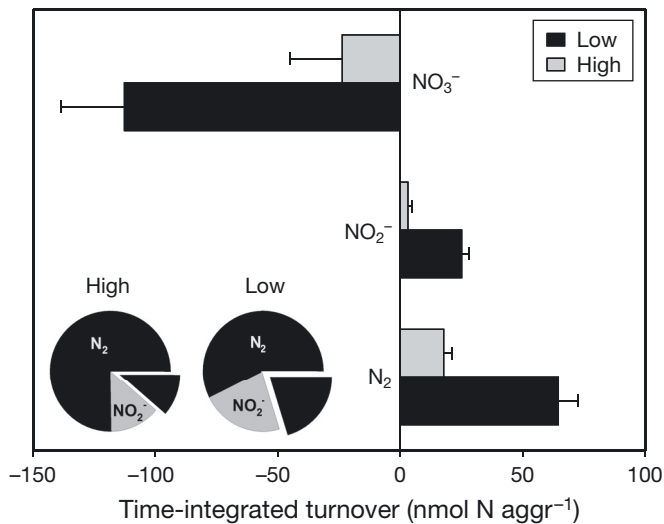
Fig. 4. Aggregate-specific, time-integrated turnover (mean ± SE, n = 3, time = 4 d) of NO_3^-, NO_2^-, and N_2 from sinking *Skeletonema marinoi* aggregates at 15% (Low) and 70% (High) O_2 AS. Positive and negative rates correspond to production and consumption, respectively. The percentage turnover of NO_3^- to NO_2^- and N_2 is depicted in a pie chart for low and high ambient O_2 levels. The 'detached' piece represents the NO_3^- not retrieved as any of the measured N species
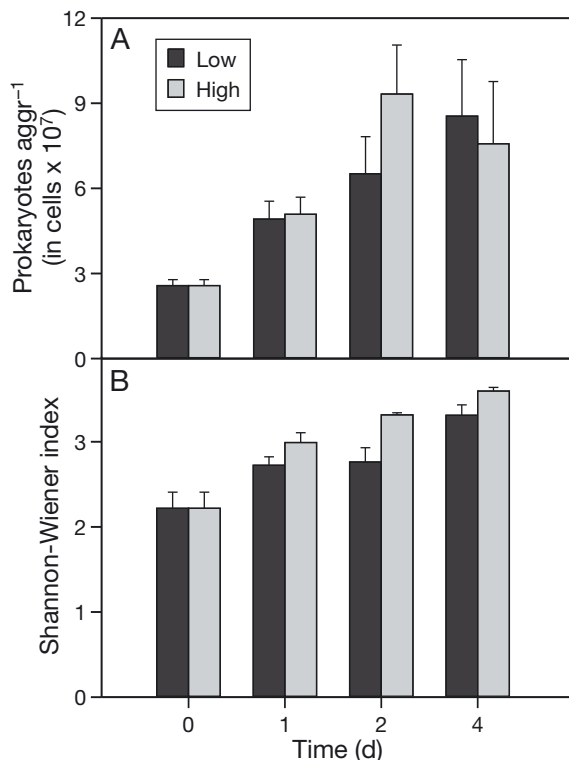

Fig. 5. (A) *Skeletonema marinoi* aggregate-associated prokaryote abundance per aggregate (mean ± SE, n = 3) at 15% (Low) and 70% (High) AS O_2 levels during 4 d. (B) Shannon-Wiener index representing the diversity of the aggregate-associated bacterial communities as derived from the same incubations

both O_2 treatments, and overall, the prokaryotic abundance in the 2 treatments increased approximately 3-fold during the 4 d of the succession experiment (Fig. 5A). The diversity of the bacterial community at the different time points was assessed with the Shannon-Wiener index using the T-RFLP data (Fig. 5B). In the high O_2 treatment, diversity increased gradually as expressed by a significant difference between subsequent time points (Table S2). This was not as distinct in the low O_2 treatment, where subsequent time points were not significantly different, but the diversity still increased significantly from T_{0d} to T_{4d}. (Fig. 5B, Table S2).

The dissimilarity of the bacterial communities between the samples was assessed with an NMDS analysis of the T-RFLP data. All 4 NMDS plots have low stress values of 0.10, 0.06, 0.06, and 0.07 (Fig. 6), indicating a high quality of the plots, but also that the bacterial communities were similar between samples (Quinn & Keough 2002). When plotting all data together (Fig. 6A), the microbial communities clustered into the following 4 groups: aggregates; natural seawater (aged); seawater from the aggregate production; and seawater from the incubations. Replicates clustered closely together, confirming homogeneity in bacterial community composition between replicates. The similarities between the 2 main clusters (seawater vs. aggregates) were assessed with ANOSIM and the significant R-score for the grouping of aggregates vs. seawater was 0.74, indicating that the 2 clusters were indeed different (Table 1). Together with the results of the control incubations, this indicates that the aggregate-associated processes were mainly driven by aggregate-specific bacterial communities and not by the communities originally found in the seawater. With respect to R-score and grouping in the 2 different O_2 treatments, time had a stronger influence at high O_2 compared to the low O_2 treatment, as indicated by R-scores of 0.72 and 0.39, respectively (Table 1, Fig. 6B,C). Furthermore, the directions of the time, diversity, and abundance vectors are roughly similar for both treatments (all vectors are significant, p < 0.05; Fig. 6B,C). When aggregates from the high and low O_2 treatments are analyzed together, it is evident from both the NMDS plot and ANOSIM that time was a strong influential factor (R-score = 0.41) with respect to the clustering of the microbial communities (Table 1, Fig. 6D). On the contrary, the R-score for grouping by the ambient O_2 concentration (low vs. high O_2) was negative and not significant, but when time was additionally taken into account (low O_2 T_{1d}, high O_2 T_{1d}, low O_2 T_{2d}, etc.), the R-score of 0.59 was significant (Table 1, Fig. 6D).
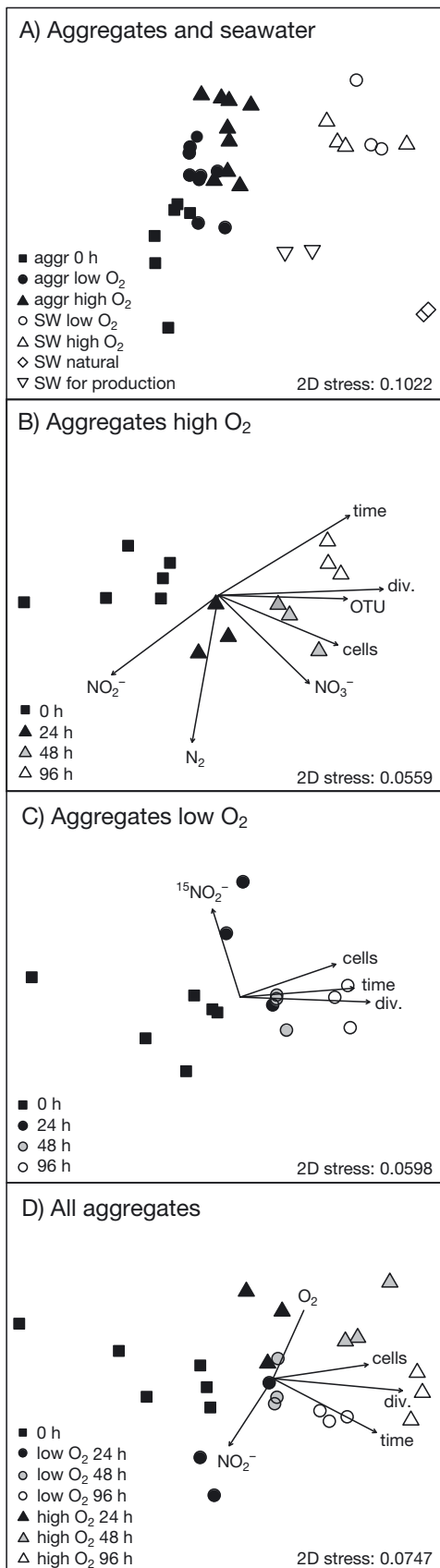
Fig. 6. Multivariate statistical analysis of microbial community structure based on terminal restriction fragment length polymophism (T-RFLP) data. (A) Dissimilarities between aggregates and seawater (SW), aging aggregates (time = 4 d) in (B) 70% (high) O_2 AS, or (C) 15% (low) O_2 AS. (D) All aggregates were analyzed with the Bray-Curtis index and plotted with NMDS. The plots were overlaid with vectors for environmental parameters (div., diversity; cells, prokaryotic abundance). Only vectors with $p < 0.05$ are shown. 2D stresses are shown

The temporal development in the microbial communities in both treatments was also evidenced by shifts in relative abundances of OTUs during the course of the experiment (Fig. 7). Specific OTUs generally exhibited similar dynamics among replicates, as can be observed in the heat map of Fig. S2. Overall, we observed a total of 82 aggregate-associated OTUs where 9 new OTUs appeared during the experiment. Most OTUs exhibited similar dynamics in the 2 parallel O_2 treatments. However, 15 and 11 OTUs (of which 10 were shared) increased more than 10-fold in relative abundance over the 4 d in the high and low O_2 treatments, respectively, while 14 and 6 OTUs (of which 3 were shared) concurrently were reduced to 1/10 or less in relative abundance. Of those, 8 and 5 were completely lost in the high and low O_2 treatments, respectively (Fig. 7), and consequently 65 and 68 OTUs, respectively, persisted throughout the incubations. Overall shifts in community structure as expressed by an extreme increase or decrease in relative abundance of given OTUs were thus most explicit in the high O_2 treatment.

DISCUSSION

Aggregate-associated O_2 and NO_3^- respiration

The O_2 and NO_3^- consumption rates of the aging diatom aggregates remained constant during the 4 d investigation. Previous studies demonstrate how exo- and ectoenzymes of the aggregate-associated bacteria hydrolyze the particulate organic carbon (POC), maintaining a high internal concentration of DOC (Azam et al. 1990, Smith et al. 1992). DOC is then subject to further microbial degradation or might be lost to the ambient seawater. Studies on phycodetrital aggregates suggest that 40 to 50% of the initial POC content is lost during a period of 3 to 6 d (Ploug & Grossart 2000, Grossart & Ploug 2001), and the decomposition rate of 0.6 to 0.9 µmol d^{-1} of aggregate-associated POC would lead to an estimated total

Table 1. ANOSIM (NMDS statistics) showing the R-score and the associated p-value for each grouping of the bacterial communities of either *Skeletonema marinoi* aggregates or seawater. Aggr., aggregates; SW, seawater; nat. SW, natural seawater; prod., production; incub., incubation; ns, not significant

| Samples	Grouping	Categories	R	p
Aggr. + SW	Aggr. or SW	Aggr., SW	0.6559	0.001
Aggr. + SW	Aggr. or SW	Aggr., nat. SW, SW from aggr. prod., SW from incub.	0.7377	0.001
Aggr. – low	Time	T_{0d}, T_{1d}, T_{2d}, and T_{4d}	0.3591	0.005
Aggr. – high	Time	T_{0d}, T_{1d}, T_{2d}, and T_{4d}	0.716	0.001
Aggr.	O_2	Low and high	ns	ns
Aggr.	Time	T_{0d}, T_{1d}, T_{2d}, and T_{4d}	0.414	0.001
Aggr.	O_2 + time	Low + T_{0d}, low + T_{1d}, low + T_{2d}, low + T_{4d}, High + T_{0d}, high + T_{1d}, high + T_{2d}, and high + T_{4d}	0.5937	0.001
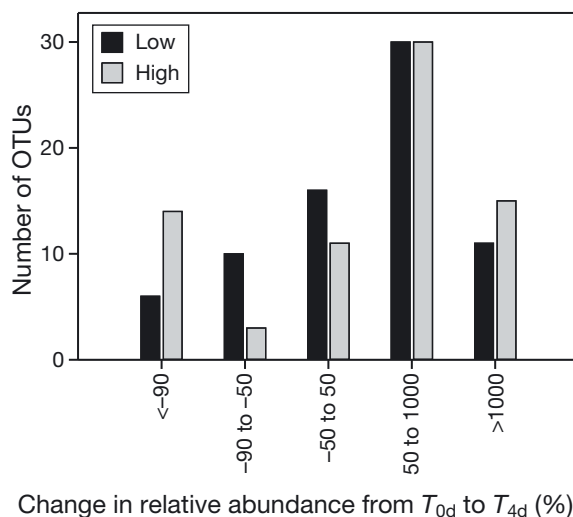
Fig. 7. Intervals of percentage change in relative abundance of aggregate-associated OTUs from T_{0d} to T_{4d} at either 15 or 70% O_2 AS (see the Supplement at www.int-res.com/articles/suppl/a079p085_supp.pdf for heat maps of all 82 OTUs)

turnover of aggregate POC in the range of 2 to 11 d (Ploug & Grossart 2000, Goldthwait et al. 2005). Therefore, the relatively constant rates of aerobic respiration and nitrate consumption observed in this study are remarkable, and indicate a steady supply of labile DOC that was sufficient to sustain constant microbial respiration for a total of 4 d. However, the O_2 consumption rates in the low O_2 treatment were 2.8 times lower than in the high O_2 treatment. As the K_m value for O_2 of microbial O_2 respiration is in the low micromolar to nanomolar range (Devol 1978, Tiano et al. 2014), O_2 consumption rates are not expected to be affected substantially by a reduction of O_2 levels from 70 to 15% AS. Potentially, solutes other than NO_3^- were reduced in the anoxic center of the aggregates. If the reduced solutes were not released to the surrounding water, or were only

slowly reoxidized in the water, they may have contributed to the observed difference in O_2 consumption. For instance, it has previously been found that model aggregate-associated Fe(III) reduction resulted in a net release of Fe(II) to the surrounding water (Balzano et al. 2009). The Fe(II) was only slowly reoxidized by the available O_2, presumably due to, for example, adhesion to organic chelates (Balzano et al. 2009). Moreover, the difference presumably reflects a larger anoxic volume in the aggregate center at low ambient O_2 levels, consistent with intensified dissimilatory nitrate reduction in these conditions. The reduced O_2 consumption in the low O_2 treatment also implies a slower turnover of labile organic carbon and hence a slower potential decay of activity at the reduced ambient O_2 levels. The elevated consumption of NO_3^- in the low O_2 treatment corresponds to ~1/20 of the difference in the O_2 consumed at low vs. high ambient O_2, and would only marginally have affected the organic carbon pool.

The higher ambient O_2 availability in the high O_2 treatment facilitated a more oxygenated interior of the aggregates and thereby enhanced the aggregate-associated labile organic carbon consumption. However, the production of N_2 and the transient accumulation of NO_2^- imply that the centers of the aggregates were, in fact, still strongly depleted in O_2, especially during the initial stages of the high ambient O_2. The production of N_2 and NO_2^- at high O_2 declined from Day 1 and ceased at Day 4 (Fig. 3C,D), presumably as the volume with strong O_2 depletion diminished along with the declining pool of labile DOC.

While we did not document anoxia in the aggregates directly, previous O_2 microsensor measurements of the O_2 distribution demonstrated internal anoxia in sinking phycodetrital aggregates; *Skeletonema marinoi* model aggregates, similar to the ones investigated here, exhibited completely anoxic centers at 15 and 40% O_2 AS, while centers were

hypoxic (~100 µM O_2) at an ambient O_2 level corresponding to 70% AS (Stief et al. 2016). In large natural cyanobacterial aggregates ($\varnothing \approx 4.7$ mm), the anoxic center expanded from 5 to 95% of the aggregate volume when the ambient O_2 AS level was decreased from 100 to 30% (Klawonn et al. 2015).

The present study shows that diatom aggregates may support NO_3^- reduction and denitrification even at 70% AS, but also that strongly O_2-depleted conditions in the aggregate interior, which are required to support these processes, were presumably only ephemeral at high ambient O_2 levels. In contrast, strongly O_2-depleted or anoxic conditions prevailed for all 4 d at low ambient O_2 levels. The observations clearly confirm that intense internal anaerobic N cycling occurs in such aggregates and that the net activity represents a sink for bioavailable nitrogen, but also a source of NO_2^-.

Anaerobic N cycling in sinking and aging diatom aggregates

Denitrification was the dominant pathway of dissimilatory nitrate reduction. We exclude a significant contribution from anammox based on the isotope pairing in ^{15}N-labeled N_2, with $^{30}N_2$ rather than $^{29}N_2$ being the main gaseous product, and because populations of anammox bacteria are not expected to be able to establish in relatively short experiments, being obligate anaerobes and having notoriously low growth rates (Strous et al. 1999). In contrast, denitrifiers are typically facultative anaerobes, fast growing, and can change metabolism depending on the availability of O_2 and NO_3^- (Zumft 1997). Dissimilatory NO_3^- reduction to NH_4^+ (DNRA) was also not an important pathway as the $^{15}NH_4^+$ accumulation was negligible during the incubations. The significant release of NO_2^-, corresponding to ~29 and 41% of the N_2 production in low and high O_2 treatments, respectively, was intriguing. Many microbes are only able to perform dissimilative NO_3^- reduction to NO_2^- (DNRN) and lack the ability to further reduce NO_2^-, and net production of NO_2^- may simply reflect an uncoupling of NO_3^- and NO_2^- reduction within the aggregate, as also observed in anoxic waters (Lam et al. 2009). The release of NO_2^- from diatom aggregates could be an important biogeochemical feature of sinking aggregates, supplying free-living communities, for example of anammox bacteria, with NO_2^-, if aggregates sink through oxygen-depleted waters. Stief et al. (2016) also found high volume-specific N_2 and NO_2^- production rates in diatom aggregates at

15% O_2 AS. Klawonn et al. (2015) documented N_2 production by relatively large cyanobacterial aggregates ($\varnothing \approx 4.7$ mm) at 30 and 100% O_2 AS, but the rates were more than an order of magnitude lower than measured here, with DNRA being the main pathway of dissimilatory NO_3^- reduction. $S.$ $marinoi$ cultures are able to perform DNRA under dark and anoxic conditions by reducing an accumulated intracellular storage of nitrate ($ICNO_3^-$) (Kamp et al. 2016). However, when associated with aggregates, $S.$ $marinoi$ apparently exhibits very low to negligible DNRA (Kamp et al. 2016). It rather appears that the lysis of aggregate-associated $S. marinoi$ supplies the microbial community within the aggregates with NO_3^-. $^{28}N_2$ ($^{14}N^{14}N$) production accounted for 21 to 31% of total N_2 production during the incubations, and isotope pairing calculations show that 8 to 13% of this $^{28}N_2$ production cannot be explained from the $^{14}NO_3^-$ background concentration in the seawater. This fraction could represent an internal supply of $^{14}NO_3^-$ being released by the diatoms.

Microbial colonization and succession in sinking and aging aggregates

The majority of bacterial colonization of aggregates presumably takes place in the photic zone (Knoll et al. 2001, Kiørboe et al. 2003, Thiele et al. 2015) and little de $novo$ colonization is anticipated to occur at greater depth (Thiele et al. 2015). However, aggregate-associated and free-living communities are shown to be fundamentally different, in both marine (DeLong et al. 1993, Rath et al. 1998, Moeseneder et al. 2001) and limnic (Crump et al. 1999, Allgaier & Grossart 2006) settings. In our study, the aggregates were formed in surface water to mimic the natural microbial colonization process. However, when the aggregates were harvested for the incubations after 3 d, the aggregate-associated bacterial communities were already different from the bacterial community in the ambient surface water (Fig. 6A, Table 1). This difference increased throughout the incubations, indicating further changes in the microbial community. Furthermore, the microbial communities within replicate aggregates became more similar with time. Therefore, time and, to a lesser extent, O_2 seem to be strong selective forces with respect to microbial succession in our incubations. The influence of O_2 becomes especially clear when considering the last 2 sampling time points (T_{2d} and T_{4d}), where the communities clustered with respect to not only time, but also O_2 level (Fig. 6D).

The unexpected finding that anaerobic N cycling in the low O_2 treatment remained unaffected by the succession in the bacterial community within the aggregates indicates functional redundancy by the developing community. Considering that many different bacteria are capable of denitrification and DNRN (Tiedje 1988, Zumft 1997, Seitzinger et al. 2006), it is possible that changes in the amount and type of POC and DOC could diversify the internal microniches, but without affecting the overall rates of anaerobic N cycling.

The bacterial communities in the center and the outer layers of the aggregates could also exhibit different patterns of development. An indication for such differences is that, besides time, also the level of O_2 drove the microbial succession in our study (Fig. 6D). Generally, the same OTUs demonstrated the most extreme changes at both high and low O_2, but they were, surprisingly, more pronounced at high O_2 (Fig. 7; see Fig. S2 in the Supplement at www.int-res.com/articles/suppl/a079p085_supp.pdf). Here, a larger part of the outer layer of the aggregate remained oxic, leading to a higher carbon oxidation rate and a more pronounced selection for bacterial taxa capable of capitalizing energy from a range of organics, including both labile and more refractory

material. Species belonging to the *Cytophaga/Flavobacteria* cluster and the *Gammaproteobacteria* are likely candidates, as they are shown to be among the dominant particle- and aggregate-associated bacteria (Ploug et al. 1999, Grossart et al. 2005, Balzano et al. 2009, Simon et al. 2014) and to increase their abundance over time in aggregates (Grossart & Ploug 2000).

Characteristics of the model aggregates

Most experimental studies on marine snow have been performed on artificially produced aggregates (model aggregates), providing standard material for manipulative investigations. However, the characteristics of both model aggregates and *in situ* aggregates vary considerably among studies and can challenge cross-study comparisons as well as extrapolation to natural conditions. In Table 2, we have compiled relevant information on model and *in situ* phycodetrital aggregates from a range of different studies and environments.

Overall, investigated phycodetrital model aggregates have diameters ranging from 1.5 to >20 mm and sinking speeds that span 45 to 1055 m d^{-1}, with

Table 2. Key characteristics of phycodetrital aggregates as presented or derived from *in situ* and model studies. See the original articles for SD or SE. ESD, equivalent spherical diameter. –: key characteristic was not specified

Aggregate constituents	Size (diameter; mm)	Size (volume; mm^3)	Sinking speed (m d^1)	Excess density (µg cm^3)	C:N (molar) –	Reference
Marine model aggregates						
Diatoms	2.2 × 1.6 × 1.6	3.1	374	2.6	7.3	This study
Diatoms	6.1 × 4.0 × 3.0	42	1055	–	–	Stief et al. (2016)
Diatoms	2.0–2.9 (ESD)	6.3-12.5	59–117	–	6.4–8.2	Ploug & Bergkvist (2015)
Diatoms and resuspended fluff particles	1.0–2.4	–	518.4	–	9.3[a]	Ziervogel & Forster (2005)
Diatoms	1–7 (ESD)	–	<750	<6.5	4.5[a]	Iversen & Ploug (2013)
Diatoms	2.5 (ESD)		113	0.2–10	–	Iversen & Ploug (2010)
Diatoms	2.6–5.9	–	45–170	–	–	Ploug (2001)
Diatoms	–	1–40	50–172	–	7.7	Ploug & Grossart (2000)
Diatoms	>20 (ESD, max. value)	–	–	–	–	Grossart et al. (2006)
Marine *in situ* aggregates						
Nodularia spumigena (cyanobacteria)	4.7	60	–	–	4.6	Klawonn et al. (2015)
Diatom dominated	1.6–9.5	–	50–180	–	–	Ploug (2001)
Diatom dominated	–	3.4 and 247.0	–	–	12.3 and 12.4	Grossart et al. (2003)
Diatom dominated	–	0.7-600	–	–	6.5–8.5[a]	Alldredge (1998)
Diatom dominated	2.4–7.5	–	74	0.01–22.00	–	Alldredge & Gotschalk (1988)
***In situ* sea-ice aggregates**						
Pennate diatom dominated	10–150	–	–	–	8–35	Fernández-Méndez et al. (2014)
Melosira filaments	10–300	–	–	–	9–40	Fernández-Méndez et al. (2014)
Pennate diatom dominated	8.7–10.4	–	–	–	8–11[a]	Assmy et al. (2013)

[a]C:N ratio is calculated from the given POC and particulate organic nitrogen (PON) values in the article

the majority of the sizes and sinking speeds in the low to intermediary range (Table 2). When considering large aggregates formed below melting sea ice, the size range of *in situ* phycodetrital aggregates tends to be larger than model aggregates (Table 2). However, the sinking speeds of natural aggregates, 50 to 180 m d^{-1}, tend to be lower than those of model aggregates, presumably due to less compaction of the associated biomass (Table 2). Nonetheless, studies report deposited fresh aggregates/diatom material at depths to >4000 m, arguing for fast sinking speeds of natural aggregates (Pfannkuche 1993, Boetius et al. 2013, Oguri et al. 2013). For instance, Agusti et al. (2015) estimated that to deliver the amount of living diatom cells observed at 3000 m depth, the sinking speed of natural aggregates needs to be 208 to 732 m d^{-1}.

The C:N ratio of model aggregates generally ranges between 4.5 and 9.3 (Table 2). For natural aggregates, the variation is larger, from 4.6 and to up to 40 (Table 2), reflecting a high degree of variation in the organic material forming natural aggregates, and in some cases, contributions of more refractory, N-depleted material.

The size, sinking speed, and C:N ratio of the model aggregates used in the present study are generally comparable to the values of model aggregates from previous investigations, but are also within the reported ranges of many *in situ* aggregates. It should, however, be acknowledged that given the relatively few *in situ* investigations on aggregates, it remains an open question to what extent the reported values reflect the actual range or even the average characteristics of aggregates in the vast, global ocean.

The present model study contributes to the previous finding that sinking *S. marinoi* aggregates can be sinks for bioavailable N and sources of NO_2^-. It demonstrates that the anaerobic processes may even be active, albeit ephemeral, at high ambient oxygen, and we show, for the first time, that the activity can be sustained for several days at low ambient oxygen levels. These findings further strengthen the hypothesis that diatom aggregates play an integral and important role for pelagic N cycling, especially in O_2-depleted environments where they may substantially contribute to N loss. However, natural aggregates are highly variable in size and composition, and they are exposed to changing environmental conditions during their descent. This is expected to affect their microbial community structure and their metabolic performance (DeLong et al. 2006, Nagata et al. 2010, Tamburini et al. 2013). Clearly, there is a need to investigate microbial processes in natural aggre-

gates, but also to better accommodate and assess the importance of changing environmental drivers during aggregate descent, such as O_2 availability, temperature, and hydrostatic pressure, which are expected to affect biogeochemical processing and microbial succession in phycodetrital aggregates.

LITERATURE CITED

Agusti S, González-Gordillo JI, Vaqué D, Estrada M and others (2015) Ubiquitous healthy diatoms in the deep sea confirm deep carbon injection by the biological pump. Nat Commun 6:7608

Alldredge A (1998) The carbon, nitrogen and mass content of marine snow as a function of aggregate size. Deep-Sea Res A 45:529–541

Alldredge AL, Cohen Y (1987) Can microscale chemical patches persist in the sea? Microelectrode study of marine snow, fecal pellets. Science 235:689–691

Alldredge AL, Gotschalk C (1988) *In situ* settling behavior of marine snow. Limnol Oceanogr 33:339–351

Alldredge A, Youngbluth M (1985) The significance of macroscopic aggregates (marine snow) as sites for heterotrophic bacterial production in the mesopelagic zone of the subtropical Atlantic. Deep-Sea Res A 32: 1445–1456

Allgaier M, Grossart HP (2006) Seasonal dynamics and phylogenetic diversity of free-living and particle-associated bacterial communities in four lakes in northeastern Germany. Aquat Microb Ecol 45:115–128

Anderson JJ, Okubo A, Robbins AS, Richards FA (1982) A model for nitrate distributions in oceanic oxygen minimum zones. Deep-Sea Res A 29:1113–1140

Assmy P, Ehn JK, Fernández-Méndez M, Hop H and others (2013) Floating ice-algal aggregates below melting arctic sea ice. PLOS ONE 8:e76599

Azam F, Cho BC, Smith DC, Simon M (1990) Bacterial cycling of matter in the pelagic zone of aquatic ecosystems. In: Tilzer MM, Serruya C (eds) Large lakes. Springer, Berlin, p 477–488

Balzano S, Statham PJ, Pancost RD, Lloyd JR (2009) Role of microbial populations in the release of reduced iron to the water column from marine aggregates. Aquat Microb Ecol 54:291–303

Boetius A, Albrecht S, Bakker K, Bienhold C and others (2013) Export of algal biomass from the melting Arctic sea ice. Science 339:1430–1432

Bower CE, Holm-Hansen T (1980) A salicylate-hypochlorite method for determining ammonia in seawater. Can J Fish Aquat Sci 37:794–798

Braman RS, Hendrix SA (1989) Nanogram nitrite and nitrate determination in environmental and biological materials by vanadium(III) reduction with chemiluminescence detection. Anal Chem 61:2715–2718

Codispoti LA, Brandes JA, Christensen JP, Devol AH, Naqvi SWA, Paerl HW, Yoshinari T (2001) The oceanic fixed nitrogen and nitrous oxide budgets: moving targets as we enter the anthropocene? Sci Mar 65:85–105

Crump BC, Armbrust EV, Baross JA (1999) Phylogenetic analysis of particle-attached and free-living bacterial communities in the Columbia River, its estuary, and the adjacent coastal ocean. Appl Environ Microbiol 65:3192–3204

Dalsgaard T, Thamdrup B, Farias L, Revsbech NP (2012) Anammox and denitrification in the oxygen minimum zone of the eastern South Pacific. Limnol Oceanogr 57: 1331–1346

DeLong EF, Franks DG, Alldredge AL (1993) Phylogenetic diversity of aggregate-attached vs. free-living marine bacterial assemblages. Limnol Oceanogr 38:924–934

DeLong EF, Preston CM, Mincer T, Rich V and others (2006) Community genomics among stratified microbial assemblages in the ocean's interior. Science 311:496–503

Devol A (1978) Bacterial oxygen-uptake kinetics as related to biological processes in oxygen deficient zones of oceans. Deep-Sea Res 25:137–146

Fernández-Méndez M, Wenzhöfer F, Peeken I, Sørensen HL, Glud RN, Boetius A (2014) Composition, buoyancy regulation and fate of ice algal aggregates in the central Arctic Ocean. PLOS ONE 9:e107452

Glud RN, Rysgaard S, Turner G, McGinnis DF, Leakey RJG (2014) Biological- and physical-induced oxygen dynamics in melting sea ice of the Fram Strait. Limnol Oceanogr 59:1097–1111

Glud RN, Grossart HP, Larsen M, Tang KW and others (2015) Copepod carcasses as microbial hot spots for pelagic denitrification. Limnol Oceanogr 60:2026–2036

Goldthwait SA, Carlson CA, Henderson GK, Alldredge AL (2005) Effects of physical fragmentation on remineralization of marine snow. Mar Ecol Prog Ser 305:59–65

Grossart HP, Ploug H (2000) Bacterial production and growth efficiencies: direct measurements on riverine aggregates. Limnol Oceanogr 45:436–445

Grossart HP, Ploug H (2001) Microbial degradation of organic carbon and nitrogen on diatom aggregates. Limnol Oceanogr 46:267–277

Grossart HP, Hietanen S, Ploug H (2003) Microbial dynamics on diatom aggregates in Oresund, Denmark. Mar Ecol Prog Ser 249:69–78

Grossart HP, Levold F, Allgaier M, Simon M, Brinkhoff T (2005) Marine diatom species harbour distinct bacterial communities. Environ Microbiol 7:860–873

Grossart HP, Czub G, Simon M (2006) Algae–bacteria interactions and their effects on aggregation and organic matter flux in the sea. Environ Microbiol 8:1074–1084

Iversen MH, Ploug H (2010) Ballast minerals and the sinking carbon flux in the ocean: carbon-specific respiration rates and sinking velocity of marine snow aggregates. Biogeosciences 7:2613–2624

Iversen MH, Ploug H (2013) Temperature effects on carbon-specific respiration rate and sinking velocity of diatom aggregates — potential implications for deep ocean export processes. Biogeosciences 10:4073–4085

Kamp A, de Beer D, Nitsch JL, Lavik G, Stief P (2011) Diatoms respire nitrate to survive dark and anoxic conditions. Proc Natl Acad Sci USA 108:5649–5654

Kamp A, Stief P, Bristow LA, Thamdrup B, Glud RN (2016) Intracellular nitrate of marine diatoms as a driver of anaerobic nitrogen cycling in sinking aggregates. Front Microbiol 7:1669

Kempers AJ, Kok CJ (1989) Re-examination of the determination of ammonium as the indophenol blue complex using salicylate. Anal Chim Acta 221:147–155

Kiørboe T, Tang K, Grossart HP, Ploug H (2003) Dynamics of microbial communities on marine snow aggregates: colonization, growth, detachment, and grazing mortality of attached bacteria. Appl Environ Microbiol 69: 3036–3047

Klawonn I, Bonaglia S, Bruchert V, Ploug H (2015) Aerobic and anaerobic nitrogen transformation processes in N_2-fixing cyanobacterial aggregates. ISME J 9:1456–1466

Knoll S, Zwisler W, Simon M (2001) Bacterial colonization of early stages of limnetic diatom microaggregates. Aquat Microb Ecol 25:141–150

Lam P, Lavik G, Jensen MM, van de Vossenberg J and others (2009) Revising the nitrogen cycle in the Peruvian oxygen minimum zone. Proc Natl Acad Sci USA 106: 4752–4757

Liu WT, Marsh TL, Cheng H, Forney LJ (1997) Characterization of microbial diversity by determining terminal restriction fragment length polymorphisms of genes encoding 16S rRNA. Appl Environ Microbiol 63: 4516–4522

McIlvin MR, Altabet MA (2005) Chemical conversion of nitrate and nitrite to nitrous oxide for nitrogen and oxygen isotopic analysis in freshwater and seawater. Anal Chem 77:5589–5595

Moeseneder MM, Winter C, Herndl GJ (2001) Horizontal and vertical complexity of attached and free-living bacteria of the eastern Mediterranean Sea, determined by 16S rDNA and 16S rRNA fingerprints. Limnol Oceanogr 46:95–107

Nagata T, Tamburini C, Arístegui J, Baltar F and others (2010) Emerging concepts on microbial processes in the bathypelagic ocean — ecology, biogeochemistry, and genomics. Deep-Sea Res II 57:1519–1536

Nielsen LP (1992) Denitrification in sediment determined from nitrogen isotope pairing. FEMS Microbiol Ecol 86: 357–362

Oguri K, Kawamura K, Sakaguchi A, Toyofuku T and others (2013) Hadal disturbance in the Japan Trench induced by the 2011 Tohoku–Oki Earthquake. Sci Rep 3:1915

Oksanen J, Blanchet FG, Kindt R, Legendre P and others (2013) Multivariate analysis of ecological communities in R: vegan tutorial. R package version 1.7. www.researchgate.net/publication/275524120_Multivariate_analysis_of_ecological_communities_in_R_vegan_tutorial_R_package_version_17

Paerl HW, Bebout BM (1988) Direct measurement of O_2-depleted microzones in marine oscillatoria: relation to N_2 fixation. Science 241:442–445

Pfannkuche O (1993) Benthic response to the sedimentation of particulate organic matter at the BIOTRANS station, 47° N, 20° W. Deep-Sea Res II 40:135–149

Ploug H (2001) Small-scale oxygen fluxes and remineralization in sinking aggregates. Limnol Oceanogr 46: 1624–1631

Ploug H, Bergkvist J (2015) Oxygen diffusion limitation and ammonium production within sinking diatom aggregates under hypoxic and anoxic conditions. Mar Chem 176: 142–149

Ploug H, Grossart HP (2000) Bacterial growth and grazing on diatom aggregates: respiratory carbon turnover as a function of aggregate size and sinking velocity. Limnol Oceanogr 45:1467–1475

Ploug H, Kühl M, Buchholz-Cleven B, Jørgensen BB (1997) Anoxic aggregates — an ephemeral phenomenon in the pelagic environment? Aquat Microb Ecol 13:285−294

Ploug H, Grossart H, Azam F, Jrgensen BB (1999) Photosynthesis, respiration, and carbon turnover in sinking marine snow from surface waters of Southern California Bight: implications for the carbon cycle in the ocean. Mar Ecol Prog Ser 179:1−11

Quinn GP, Keough MJ (2002) Experimental design and data analysis for biologists. Cambridge University Press, Cambridge

Rath J, Wu KY, Herndl GJ, DeLong EF (1998) High phylogenetic diversity in a marine-snow-associated bacterial assemblage. Aquat Microb Ecol 14:261−269

Schramm A, de Beer D, Wagner M, Amann R (1998) Identification and activities *in situ* of *Nitrosospira* and *Nitrospira* spp. as dominant populations in a nitrifying fluidized bed reactor. Appl Environ Microbiol 64: 3480−3485

Seitzinger S, Harrison JA, Böhlke JK, Bouwman AF and others (2006) Denitrification across landscapes and waterscapes: a synthesis. Ecol Appl 16:2064−2090

Silver M (2015) Marine snow: a brief historical sketch. Limnol Oceanogr Bull 24:5−10

Simon H, Lipsewers YA, Giebel HA, Wiltshire KH, Simon M (2014) Temperature effects on aggregation during a spring diatom bloom. Limnol Oceanogr 59:2089−2100

Simon M, Grossart HP, Schweitzer B, Ploug H (2002) Microbial ecology of organic aggregates in aquatic ecosystems. Aquat Microb Ecol 28:175−211

Smetacek VS (1985) Role of sinking in diatom life-history cycles: ecological, evolutionary and geological significance. Mar Biol 84:239−251

Smith D, Simon M, Alldredge A, Azam F (1992) Intense hydrolytic enzyme-activity on marine aggregates and implications for rapid particle dissolution. Nature 359: 139−142

Stief P, Kamp A, Thamdrup B, Glud RN (2016) Anaerobic nitrogen turnover by sinking diatom aggregates at varying ambient oxygen levels. Front Microbiol 7:98

Strous M, Kuenen JG, Jetten MSM (1999) Key physiology of anaerobic ammonium oxidation. Appl Environ Microbiol 65:3248−3250

Tamburini C, Boutrif M, Garel M, Colwell RR, Deming JW (2013) Prokaryotic responses to hydrostatic pressure in the ocean — a review. Environ Microbiol 15:1262−1274

Thiele S, Fuchs BM, Amann R, Iversen MH (2015) Colonization in the photic zone and subsequent changes during sinking determine bacterial community composition in marine snow. Appl Environ Microbiol 81:1463−1471

Tiano L, Garcia-Robledo E, Dalsgaard T, Devol AH and others (2014) Oxygen distribution and aerobic respiration in the north and south eastern tropical Pacific oxygen minimum zones. Deep-Sea Res A 94:173−183

Tiedje JM (1988) Ecology of denitrification and dissimilatory nitrate reduction to ammonium. In: Zehnder AJB (ed) Environmental microbiology of anaerobes. John Wiley & Sons, New York, NY, p 179−244

Velji MI, Albright LJ (1986) Microscopic enumeration of attached marine bacteria of seawater, marine sediment, fecal matter, and kelp blade samples following pyrophosphate and ultrasound treatments. Can J Microbiol 32:121−126

Warembourg FR (1993) Nitrogen fixation in soil and plant systems. In: Knowles R, Paul EA, Melillo J, Blackburn H (eds) Nitrogen isotope techniques. Academic Press, San Diego, CA, p 127−156

Wörner U, Zimmerman-Timm H, Kausch H (2000) Succession of protists on estuarine aggregates. Microb Ecol 40: 209−222

Yang F, Troncy E, Francœur M, Vinet B, Vinay P, Czaika G, Blaise G (1997) Effects of reducing reagents and temperature on conversion of nitrite and nitrate to nitric oxide and detection of NO by chemiluminescence. Clin Chem 43:657−662

Ziervogel K, Forster S (2005) Aggregation and sinking behaviour of resuspended fluffy layer material. Cont Shelf Res 25:1853−1863

Zumft WG (1997) Cell biology and molecular basis of denitrification. Microbiol Mol Biol Rev 61:533−616